

COVER PAGE

Document downloaded by @DAEL

Sat Nov 28 03:29:25 2026
For personal use

When automatic English translation is provided, only the original document is authentic.
The EAA cannot be held responsible of any translation error

Bibliographical reference

Overpressure Dependence of Sub-Harmonic Generation from Contrast Agent SonoVue Microbubbles, Jun Wu, Tingbo Fan, Di Xu and Dong Zhang, Acta Acustica **vol. 101** (Number 1), 2015, pp. 55-61

DOI
https://doi.org/10.3813/AAA.918804

Acta Acustica united with Acustica
Vol. 101 (2015) 55 – 61

DOI 10.3813/AAA.918804

Overpressure Dependence of Sub-Harmonic Generation from Contrast Agent SonoVue Microbubbles

Jun Wu[1)], Tingbo Fan[2,3)], Di Xu[1)], Dong Zhang[3)]

[1)] The First Affiliated Hospital of Nanjing Medical University, Nanjing 210029, China. di_hsu@126.com

[2)] Jiangsu Province Institute for Medical Equipment Testing, Nanjing 210012, China

[3)] Institute of Acoustics, Key Laboratory of Modern Acoustics (Nanjing University), Ministry of Education, Nanjing University, Nanjing 210093, China. dzhang@nju.edu.cn

Summary

Sub-harmonic component generated from microbubbles has been proven to be potentially used in noninvasive blood pressure measurement. In the present work, the overpressure dependence of the sub-harmonic generation from a commercial ultrasound contrast agent SonoVue was theoretically and experimentally investigated with varied excitation pressure amplitudes and pulse lengths. With 4-MHz ultrasound excitation at an applied acoustic pressure amplitude of 0.2 MPa, the measured sub-harmonic amplitude exhibited a decreasing change as the overpressure increases; while non-monotonic change was observed for the applied acoustic pressures of 0.3 and 0.4 MPa, and the peak position in the curve of the sub-harmonic response versus the overpressure was shifted towards higher overpressure as the excitation pressure amplitude increases. Furthermore, the exciting pulse with long duration could lead to better sensitivity of the sub-harmonic response to the overpressure. The measured results were interpreted by the numerical simulations based on the Marmottant model. This work might provide a solid proof for the optimization of the noninvasive blood pressure measurement using sub-harmonic generation from microbubbles.

PACS no. 43.25.Dc, 43.35.Yb, 43.80.Qf

1. Introduction

Ultrasound contrast agents (UCAs) are usually comprised by suspensions of gas-filled microbubbles with micrometer diameters encapsulated by a thin stabilization coating (e.g., lipid, albumin, or polymer) [1, 2], UCAs were initially used in ultrasound medical applications to improve the quality of ultrasonic images. Besides enhancing the reflection of ultrasound, the UCA microbubbles also exhibit nonlinear vibrations under insonation, which will produce harmonic, sub-harmonic, and ultra-harmonic responses [3, 4]. In the past decades, various techniques have been proposed for noninvasive blood pressure measurements using UCA microbubbles. Fairbank and Scully developed a method for cardiac pressure measurements based on the resonant frequency of UCAs [5]. Bouakaz *et al.* proposed a technique for blood pressure measurement via the measurement of the disappearance time of free bubbles [6]. Recently, sub-harmonic response has been used for local blood pressure measurements owing to approximately linear relationship between sub-harmonic response and overpressure [7], Shi *et al.* experimentally found that the sub-harmonic response from UCA microbubbles is robustly dependent on the overpressure [8, 9]. However, the sub-harmonic responses of UCAs might exhibit different tendencies as the overpressure increases at different excitation levels. Frinking *et al.* found that the sub-harmonic response increases by 28.9 dB for 180 mm Hg increase of overpressure at a low excitation level of 50 kPa; while the sub-harmonic response exhibited a 9.6 dB decrease at a higher excitation pressure of 400 kPa [10]. Andersen and Jensen theoretically proved that the variation of sub-harmonic component should be related to the exciting parameters, such as the pulse shape, length and amplitude [11], Katiyar *et al.* indicated that the change in the sub-harmonic response is dominated by the ratio of the excitation frequency to the natural frequency of the bubble [12].

In the present study, the overpressure dependence of the sub-harmonic generation from the UCA SonoVue microbubbles at varied ultrasonic excitation conditions (viz. amplitude and pulse length) was further experimentally examined. Moreover, numerical simulations based on the Marmottant model [13] were performed to interpret the measured results.

Received 29 January 2014,
accepted 06 October 2014.

© S. Hirzel Verlag · EAA

2. Theory and methods

Various types of modified Rayleigh-Plesset (RP) equations have been developed to study microbubble dynamics in an incompressible liquid [13]. In the present study, the Marmottant model is used for describing the dynamic behavior of microbubbles encapsulated with thin lipid shell [13]. The dynamic equation of the model is written as

$$\rho R\ddot{R} + \frac{3}{2}\rho\dot{R}^2 = \left[P_0 + P_{ov} + \frac{2\sigma(R_0)}{R_0}\right]\left(\frac{R_0}{R}\right)^{3\kappa}\left(1 - \frac{3\kappa}{c}\dot{R}\right) - \left(P_0 - P_{ov}\right) - \frac{2\sigma(R)}{R} - \frac{4\mu\dot{R}}{R} - \frac{4\kappa_s\dot{R}}{R} - p_{ac}(t), \quad (1)$$

where R is the instantaneous radius of the microbubble; $\dot{R}$, $\ddot{R}$ are the first and second time derivatives of R; R_0 is the equilibrium radius; ρ is the density of the surrounding medium; κ is the polytropic exponent; μ is the surrounding liquid viscosity; κ_s is the surface dilatational viscosity; P_0 is the hydrostatic pressure; P_{ov} is the overpressure; $P_{ac}(t)$ is the exciting acoustic pressure; c is the sound velocity. The Marmottant model underlines the effective surface tension of a microbubble during its oscillation and the movement of the bubble is defined as three successive stages as the surface tension rises. The effective surface tension $\sigma(R)$ is expressed as [13]

$$\sigma(R) = \begin{cases} 0 & \text{if } R \le R_{\text{buckling}}, \\ \chi\left(\frac{R^2}{R_{\text{buckling}}^2} - 1\right) & \text{if } R_{\text{buckling}} \le R \le R_{\text{break-up}}, \\ \sigma_{\text{water}} & \text{if ruptured and} R \ge R_{\text{ruptured}}. \end{cases} \quad (2)$$

As the bubble radius is below R_{buckling}, the surface buckles and $\sigma = 0$; The elastic modulus χ gives the slope of the elastic regime where the bubble radius is between R_{buckling} and $R_{\text{break-up}}$; R_{ruptured} describes the moment of rupture and the maximum surface tension saturates at σ_{water}.

The scattered acoustic response is calculated from the radial response at a distance of d from the microbubble [14].

$$P_s(d,t) = \rho\frac{R}{d}\left(2\dot{R}^2 + R\ddot{R}\right). \quad (3)$$

Considering that UCA microbubbles have a wide size distribution, a weighting scheme [14, 15] is utilized to determine the cumulative echoes on the basis of the size distribution of microbubbles. $S(f)$ represents the total scattered pressure from microbubbles with sizes ranging from r_i to r_j at a frequency f,

$$S(f) = \left(\sum_{k=i}^{j} P_s(r_k, f)\, w_k\right) \Big/ \sum_{k=i}^{j} w_k, \quad (4)$$

where $P_s(r_k, f)$ is the scattered pressure from microbubbles with size r_k at the frequency f; w_k is the number percentage weight of bubbles with size r_k. r_i and r_j represent the minimum and maximum radii for microbubble clouds.

Table I. Parameters of SonoVue microbubbles.

Symbol	Description	Value
κ_s	shell surface dilatational viscosity	$6.5\cdot10^{-8}$ kg/s
χ	shell elastic compression modulus	1.05 N/m
σ_0	surface tension in the equilibrium	0.7 N/m
$\sigma_{\text{break-up}}$	critical tension where shell breaks	0.13 N/m
d_s	shell thickness of bubble (m)	$0.1\%\cdot R_0$
σ_{water}	water surface tension	0.072 N/m
p_0	hydrostatic pressure	$1.01\cdot10^5$ N/s^2
κ	polytropic exponent of the gas	1.4
ρ	density of surrounding liquid	998 kg/m^3
c	sound speed in liquid	1500 m/s
μ	viscous in liquid	$1.0\cdot10^{-3}$ N/m^3
R_0	equilibrium radius	2.0 µm
R_{buckling}	equilibrium radius	1.8 µm

On the other hand, note that the linear resonance frequency f_0 of a microbubble in the elastic state is

$$f_0 = \frac{1}{2\pi R_0}\sqrt{\frac{1}{\rho}\left(3\kappa P_{\text{amp}} + \frac{2\sigma(R_0)}{R_0}(3\kappa - 1)\right)}, \quad (5)$$

where $P_{\text{amp}} = P_0 + P_{ov}$. The resonance frequency depends both on ambient pressure and radius.

In the simulation, some physical constants were set as listed in Table I [16].

3. Experimental setup

SonoVue (Bracco Diagnostics Inc., Geneva, Switzerland), one of the new generation UCA commonly used in Europe and the U.S. is filled with sulfur hexafluoride (SF_6) gas encapsulated by thin lipid monolayer membrane. According to the manufacturer's instruction, the purchased SonoVue vial should be vented with a sterile 18-gauge needle, followed by 5-ml phosphate buffered saline (PBS) injection into the vial to have UCA microbubbles reconstituted. The microbubbles would be evenly distributed by inversion agitation of the vial which contained 2–5$\cdot10^8$ microbubbles/ml. During the experiments, the reconstituted SonoVue suspension would be further diluted to a predetermined volume concentration. The average radius of the encapsulated microbubbles is around 2 µm, its corresponding resonance frequency is about 2.2 MHz. The size distribution of microbubbles was measured by a Coulter Counter (Coulter Corporation, Hialeah, FL) as shown in Figure 1. The elasticity of the shell was determined by the optimization method based on the sound attenuation spectrum [16]. The determined parameters for microbubbles are listed in Table I.

For acoustic attenuation measurements shown in Figure 2a, the methods similar to those proposed by de Jong *et al.* [17] and Hoff *et al.* [16]. Two unfocused transducers of 2.25 and 5.0 MHz dominant frequencies (V325-SU and V326-SU, 0.375 in. diameter, Panametrics, Waltham,

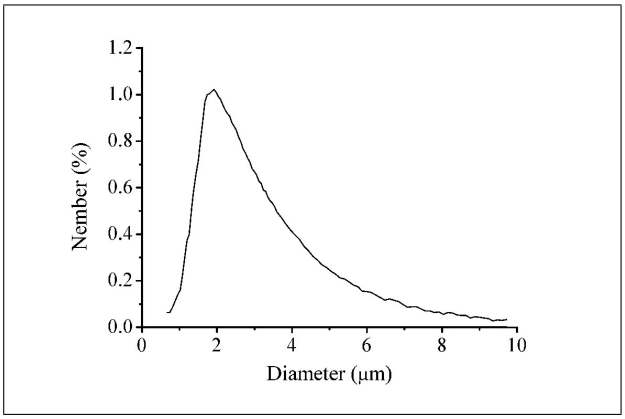

Figure 1. Size distribution of SonoVue microbubbles.

MA) were used, each as transmitter and receiver simultaneously. The −6 dB bandwidths for these two transducers are: 1.05- to 3.55-MHz for V325-SU and 2.75- to 7.1-MHz for V326-SU. The two transducers could be selected with the help of a switcher and were mounted in parallel in a water tank made of Perspex. The microbubble samples were filled in a polyamides cell of 2 cm thickness, with thin polythene membranes acting as acoustic windows, and were placed at a distance of 8 cm from the transducers. A stain steel block working as the reflector was located 8 cm from the sample. A pulser/receiver (5900PR, Panametrics, Waltham, MA) was used to drive the two transducers at 200 pulses/s and extract the reflected signals. The driving pressure of the transmitting signals was about 50 kPa, so that the UCA microbubbles would be expected to undergo linear oscillations. Each of the detected signals included 5000 data points after digitalization by the oscilloscope at a sample rate of 50MHz. In determining the transmission spectra of microbubble samples, the 2.25 MHz transducer was used between 1 and 3.5 MHz, and the 5MHz transducer covered the frequency range from 3 to 7 MHz. As suggested by Hoff *et al.* [16] ideally these two transducers should give equal measurement results within the overlapped frequency region. Therefore the two obtained transmission spectra were averaged in the overlapped frequency region. To calculate the frequency-dependent attenuation, the transmission spectrum of water was divided by that of the samples.

Figure 2b shows the diagram of the experimental setup for measuring the sub -harmonics responses scattered from UCA microbubbles. An arbitrary waveform generator (Agilent 33250, CA, USA) was used to produce 4-MHz tone-burst signals with varied pulse lengths (16, 32 or 64 cycles) at a pulse repetitive frequency (PRF) of 100 Hz. After being amplified by an RF power amplifier (A150, ENI, Rochester, NY, USA), the signals were used to drive a plane transducer (V380-SU, Panametrics, Waltham, MA, USA, center frequency = 4.0 MHz, diameter = 1 cm). The scattered wave was received by another plane transducer (V304-SU, Panametrics, Waltham, MA, USA, center frequency = 2.25 MHz diameter = 1 cm). After passing through a pre-amplifier (fixed gain of 30 dB,

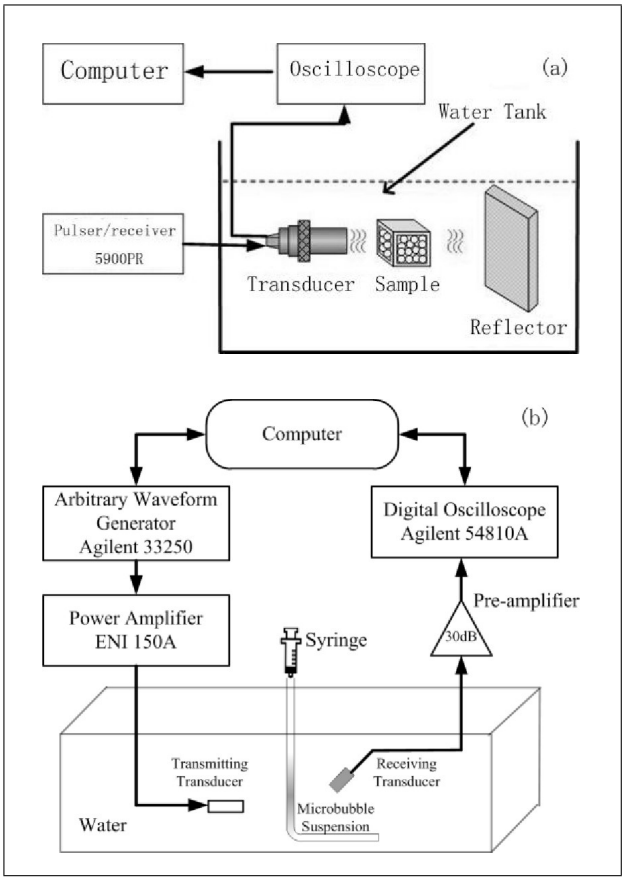

Figure 2. Experiment setups of (a) the acoustic attenuation measurement system and (b) sub-harmonic measurement system.

HPA30, NTR Systems, Inc. Seattle, WA, USA), the received signal was captured by a digital oscilloscope (Agilent 54810, Santa Clara, CA, USA). The transmitter and receiver were orthogonally positioned in order to reduce the impact of the insonating signal on the detection of the sub-harmonic signals. A plastic transparent pipe (6.0 mm outer diameter and 5.0 mm inner diameter) was used to hold the microbubble suspension. One end of the pipe was airtight, and the other end was connected with a syringe containing 50 ml air. The overpressure was controlled by changing the air volume in the syringe. A linear 3-axial scanning system (ESP7000, Newport Electronics, Inc., Santa Ana, CA, USA) controlled by a PC via a Labview software (National Instruments, Austin, TX, USA) was used for aligning the transmitter and receiver. The *in situ* acoustic pressure of the transmitting transducer was calibrated by using a needle hydrophone (TNU001A, NTR Systems, Inc. Seattle, WA, USA) with a 30-dB preamplifier (HPA30, NTR Systems, Inc. Seattle, WA, USA). All measurements were performed at room temperature (approximately 23 °C). Five replicated measurements were performed at each setting for the sub-harmonic emissions with refreshed microbubble suspensions. For each measurement, the responses of microbubbles were averaged over 100 traces and then analyzed by using a Fast-Fourier-Transform (FFT) program in MATLAB (MathWorks, Inc., Natick, WA, USA).

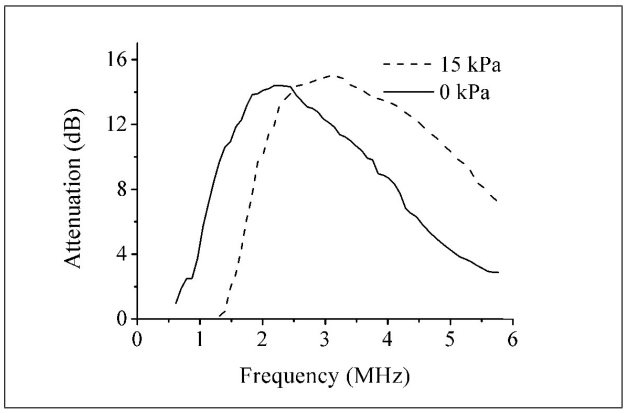

Figure 3. Attenuation spectrum of the microbubbles at overpressures of 0 and 15 kPa.

4. Results and discussion

It has been indicated that the generation of sub-harmonics occurs when the exciting acoustic pressure exceeds a certain threshold, and the threshold pressure reaches a minimum level at $f = 2f_0$ [17]. Figure 3 shows the measured attenuation spectrum for the microbubbles. When the overpressure is zero, it is seen that the resonant frequency of the microbubbles is around 2 MHz. Therefore, the exciting frequency of 4 MHz was chosen in both the simulations and the measurements. Figure 4a plots the spectrum of the signals scattered from microbubbles excited by 4-MHz ultrasound at an acoustic pressure of 0.3 MPa and pulse length of 64 cycles, where the curve is normalized to the fundamental component amplitude. Significant discrete sub-harmonic component was observed, which indicates that this frequency could be utilized to generate sufficient sub-harmonic signal. Figure 4b illustrates the amplitudes of sub-harmonic components when the exciting acoustic pressure amplitude changes from 0.05 to 0.75 MPa. It is shown that the pressure threshold for the generation of sub-harmonic responses is about 0.15 MPa. When the exciting acoustic pressure increases from 0.2 to 0.45 MPa, the amplitude of the sub-harmonic component is enhanced by 20 dB. The sub-harmonic amplitude reaches saturation as the exciting acoustic pressure exceeds 0.45 MPa. The result indicates that the sub-harmonic responses generated from microbubbles can be divided into three stages, i.e. generation, rapid-rise and saturation, which coincides well with the reported results [18, 19]. In the following experiments, microbubbles were driven by ultrasound pulses at 0.2, 0.3 and 0.4 MPa, respectively.

Figure 5 shows the dependences of sub-harmonic response on overpressure at varied exciting acoustic pressure amplitudes (Figure 5a) and pulse lengths (Figure 5b). All data points were expressed as the mean ±standard deviation (SD) of 5 replicate measurements. In Figure 5a, the pulse length was fixed as 64 cycles; while in Figure 5b, the excitation pressure was kept at 0.3 MPa. As shown in Figure 5a, the sub-harmonic amplitude *decreased* as the overpressure *increased* for the applied acoustic pressure amplitude of 0.2 MPa. However, non-monotonic changes

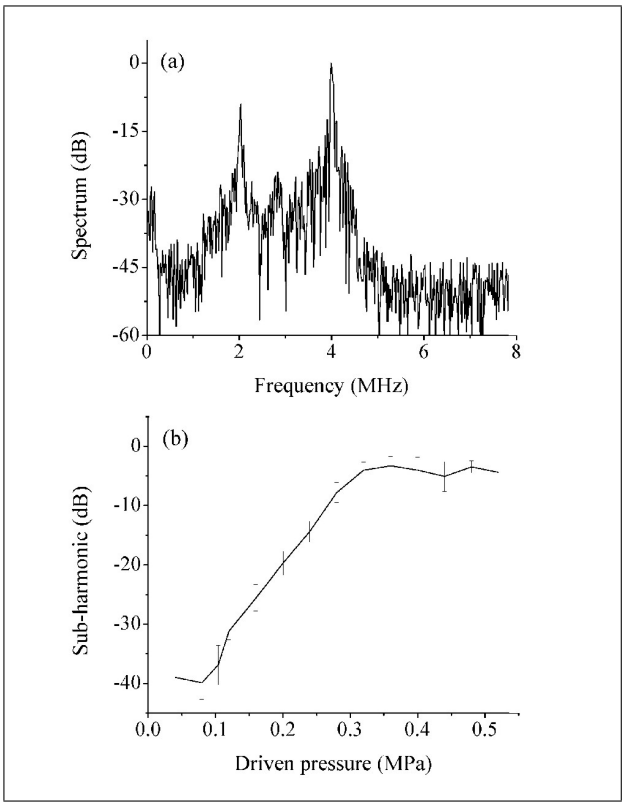

Figure 4. (a) The spectrum of the scattered signals from microbubbles, and (b) The sub-harmonic generation as a function of exciting acoustic pressure.

were observed for the applied acoustic pressures of 0.3 and 0.4 MPa. There was an increasing tendency as the overpressure increases at the initial stage; after reaching a peak, the sub-harmonic amplitude began to decrease with the increasing overpressure. In addition, the position of maximum sub-harmonic amplitude shifted towards higher overpressure for higher excitation acoustic pressure. The maximum sub-harmonic amplitudes occur at overpressures of 5.0 and 7.8 kPa corresponding to the exciting acoustic pressures of 0.3 and 0.4 MPa, respectively. The previous studies have indicated that the sub-harmonic amplitude increases or decreases monotonically with the increasing of overpressure [9, 10, 11]. The non-monotonic variation of sub-harmonic in the current study was related to the change of the resonance frequency of UCA microbubbles, which will be discussed later.

When the exciting acoustic pressure amplitude was kept at 0.3 MPa, the dependence of the sub-harmonic responses on the overpressure for varied pulse lengths is shown in Figure 5b. It is observed that for all overpressures from 0 to 25 kPa, the sub-harmonic amplitude increased when the pulse length increases from 32 cycles to 64 cycles. However, for the pulse length of 16 cycles, the sub-harmonic amplitude almost kept constant when the overpressure changes from 0 to 25 kPa. It seems that, for the ultrasound exposure with a pulse length of 16 cycles, the generation of sub-harmonic components was not sensitive to the variation of ambient pressure. It perhaps related to destruction

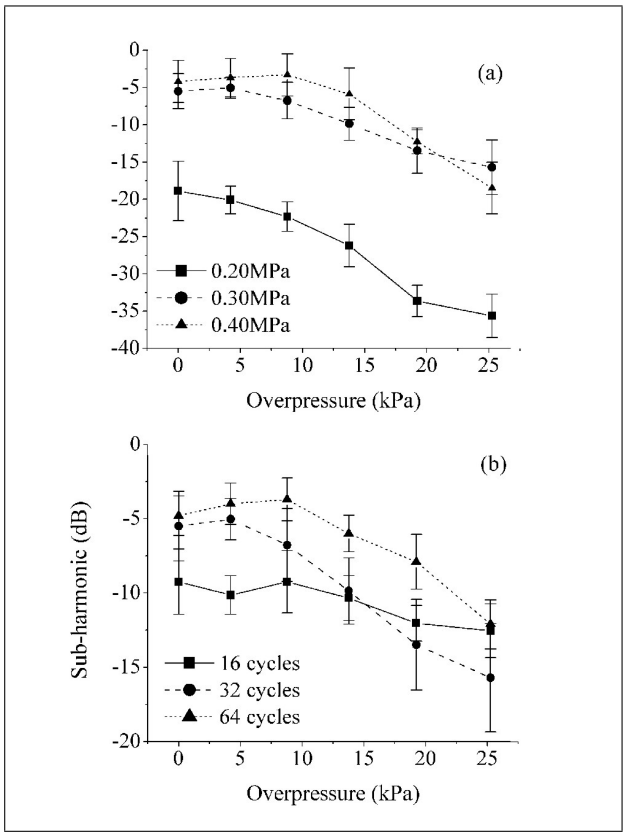

Figure 5. The dependence of sub-harmonic amplitude on overpressure for varied (a) exciting acoustic pressure and (b) pulse length.

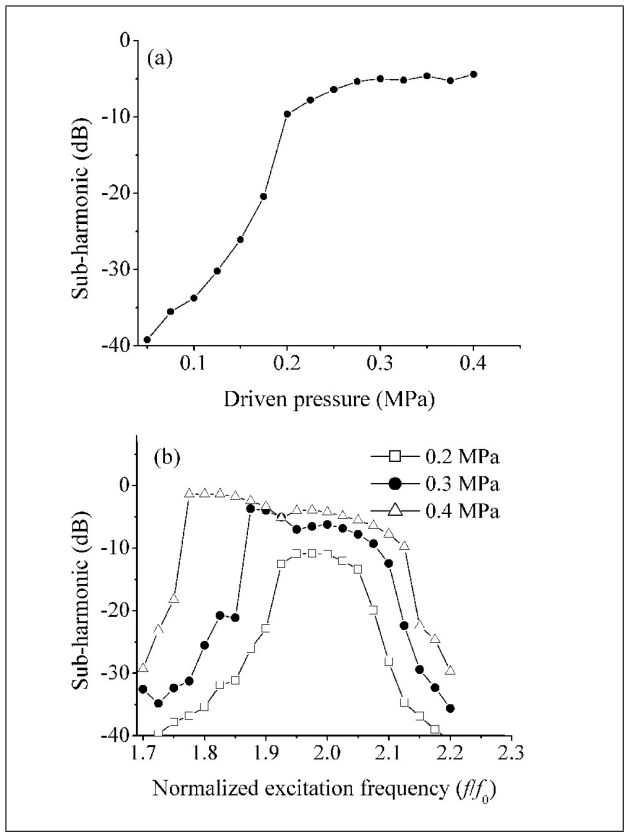

Figure 6. Calculated sub-harmonic responses as a function of (a) exciting pressure amplitude, and (b) exciting frequency.

of larger bubbles and consequent generation of smaller bubbles that respond better to 4 MHz during an individual pulse but which dissolve to smaller, inactive sizes during the experiment.

Figure 6a shows the calculated amplitudes of sub-harmonics as a function of the applied acoustic pressure at zero overpressure. As the exciting acoustic pressure increasing from 0.1 to 0.4 MPa, the sub-harmonic amplitude increased by 38 dB. The sub-harmonic amplitude reaches saturation as the driving pressure exceeds 0.2 MPa. Compared with the measured results (Figure 4b), the change tendency were qualitatively in the agreement, but the excitation pressure at which the sub-harmonics get saturation was much lower than the measured one. The possible reason might be that the simulation takes no account of the microbubble destruction.

The amplitudes of sub-harmonics were calculated as a function of exciting frequency at zero overpressure and three exciting pressure levels (viz. 0.2, 0.3 and 0.4 MPa). The calculated results are demonstrated in Figure 6b, where the exciting frequency is normalized by the resonance frequency. For simplicity, Figure 6b is calculated using the averaged radius. It is obvious that similar variation tendencies could be observed at different exciting pressure levels. For example, when the exciting acoustic pressure amplitude is 0.3 MPa, the sub-harmonic response initially increased as $f/f_0 \leq 1.85$. Then, the sub-harmonic amplitude reached a peak value at $f/f_0 = 1.85$. Non-smooth variation could be observed for the sub-harmonic amplitudes as $1.85 \leq f/f_0 \leq 2.0$, while the sub-harmonic amplitude decreased monotonically for $f/f_0 > 2.0$. As indicated by equation (5), if the overpressure increases, the microbubble resonance frequency would increase as well, leading to the reduction of f/f_0. As shown in Figure 3, as the overpressure increases from 0 to 15 kPa, the resonant frequency increases from 2.2 MHz to 3.2 MHz. If the exciting frequency satisfies $f/f_0 \leq 1.85$, the sub-harmonic amplitude would decrease with the increasing of the overpressure. Inversely, if the exciting frequency satisfies $f/f_0 \leq 2.0$, the sub-harmonic amplitude would increase with the increasing overpressure. While for $1.85 \leq f/f_0 \leq 2.0$, the curve of the sub-harmonic amplitude versus overpressure would be non-monotonic. These results provide a possible explanation to the measured change of the sub-harmonic response as a function of the overpressure. In addition, one can find in Figure 6b that the peak position of the sub-harmonic amplitudes shifted toward lower value of f/f_0 as the exciting pressure increases. The simulated results are also in agreement with the measured curves in Figure 5a, where the peaks of the sub-harmonic amplitudes occur at 5 and 7.8 kPa corresponding to the exciting acoustic pressures of 0.3 and 0.4 MPa,

Figure 7 illustrates the calculated sub-harmonic response as a function of the overpressure when the microbubble is driven by 4-MHz ultrasonic pulses with varied pressure amplitudes and pulse lengths. In Fig-

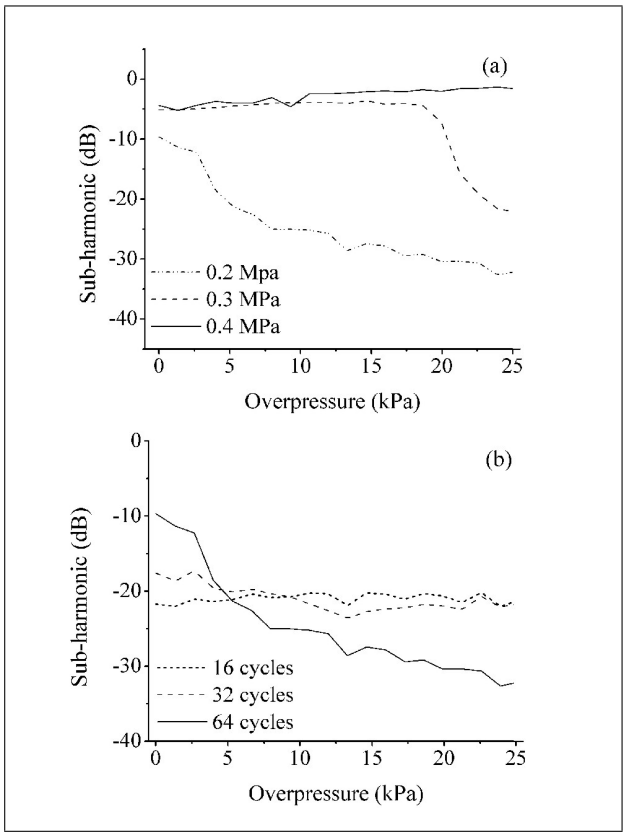

Figure 7. Calculated dependences of sub-harmonic amplitude on the overpressure for varied (a) exciting acoustic pressure amplitude, and (b) pulse length.

ure 7a, the exciting pulse length was fixed at 64 cycles. For excitation pressure amplitudes of 0.2 MPa, the sub-harmonic amplitude decreased with the increasing of overpressure. However, for the exciting pressure amplitude of 0.3 MPa, the change of sub-harmonic amplitude became non-monotonic. In this study, the driving frequency was 4 MHz, the corresponding f/f_0 was 1.81. As indicated by the curve at 0.2 MPa in Figure 6b, the sub-harmonic amplitude would decrease with the increasing of the overpressure for $f/f_0 < 1.95$. Comparing with the measured results shown in Figure 5a, the sub-harmonic amplitude shows decreasing tendency only for 0.2 MPa, which is in agreement with the simulated results.

Figure 7b shows the influence of the pulse length on the sub-harmonic response when the microbubble is driven at an acoustic pressure of 0.3 MPa. With the increasing pulse length, the sub-harmonic response becomes more sensitive to the overpressure. For the pulse of 64 cycles, the sub-harmonic amplitude decreases by about 22 dB as the overpressure changes from 0 to 25 kPa. It indicates that the pulse with longer pulse length would lead to better sensitivity for the overpressure measurement.

Previous studies have indicated that the non-invasive blood pressure measurement can be made based on either increasing or decreasing of the sub-harmonic generation from UCA microbubbles [10, 11]. In this work, it is noticed that the relationship between the sub-harmonic generation and the overpressure shows either decreasing or non-monotonic changes. The relation mainly depends on the ratio of the exciting frequency to the resonant frequency f/f_0, the exciting acoustic pressure amplitude, and the microbubble parameters. For the UCA microbubbles used in this study, the monotonic change can be derived at 4 MHz ultrasound excitation with an acoustic pressure of 0.2 MPa. When increasing the acoustic pressure, the relation will become non-monotonic. The results confirm the theoretical results obtained by Katiyar [12]. If choosing the exciting frequency close to $2f_0$, the effect of the acoustic pressure amplitude on the monotonic relationship can be reduced as indicated by Figure 6b.

Note that the variations of sub-harmonic components in the numerical simulations are more significant than the measured results. The main reason is that the model used in this study takes no account of the microbubble destruction. However, the simulated results still can provide qualitative interpretation for the experimental results. This implies that the ultrasound exciting conditions could be optimized based on this theoretical model, and it may suggest that the sensitivity achievable for noninvasive pressure measurement could be improved further by carefully tuning the microbubble parameters. This may require a contrast agent specifically designed for noninvasive pressure measurements, which will be the object of future studies.

5. Conclusion

In conclusion, the dependence of the sub-harmonic amplitude of microbubbles on the overpressure has been investigated under different acoustic driving conditions by both experimental measurements and numerical simulations. In the experiments, either decreasing or non-monotonic curves of the sub-harmonic amplitude versus the overpressure have been observed. The ratio of exciting frequency to microbubble resonance frequency and the acoustic pressure amplitude are shown to be the dominant parameters that can determine the change tendency of the sub-harmonics. The results also demonstrate that the exciting signal with longer pulse length could provide better sensitivity of the sub-harmonics to the overpressure. This study provides valuable foundation for the optimization of local blood pressure measurement using the sub-harmonic response generated from the microbubbles.

Acknowledgement

The work is supported by the National Basic Research Program 973 (Grant No. 2011CB707900) from the Ministry of Science and Technology, China, National Natural Science Foundation of China (Grant Nos. 81271589, 81127901, 81227004, 81301616, 11174141, 11374155, 11161120324), and Natural Science Foundation of Jiangsu Province (Grant No. BE2011110 and BK20131017), and the National High-Tech Research and Development Program 862 (Grant No. 2012AA022702).

References

[1] P. Frinking, A. Bouakaz, J. Kirkhom, F. Cate, N. de Jong: Ultrasound contrast imaging: current and new potential methods. Ultrasound Med. Biol. **26** (2000) 965–975.

[2] F. A. Duck: Nonlinear acoustics in diagnostic ultrasound. Ultrasound Med. Biol. **28** (2002) 1–18.

[3] N. de Jong, R. Cornet, C. T. Lancee: Higher harmonics of vibrating gas-filled microspheres. Part one: Simulations. Ultrasonics **32** (1994) 447–453.

[4] W. T. Shi, F. Forsberg: Ultrasonic characterization of the nonlinear properties of contrast microbubbles. Ultrasound Med. Biol. **26** (2000) 93–104.

[5] W. M. Fairbank, M. O. Scully: New noninvasive technique for cardiac pressure measurement-resonant scattering of ultrasound from bubbles. IEEE Trans. Biomed. Eng. **24** (1977) 107–110.

[6] A. Bouakaz, P. J. A. Frinking, N. de Jong, N. Bom: Noninvasive measurement of the hydrostatic pressure in a fluid-filled cavity based on the disappearance time of micrometer-sized free gas bubbles. Ultrasound Med. Biol. **25** (1999) 1407–1415.

[7] F. Forsberg, J. B. Liu, W. T. Shi, J. Furuse, M. Shimizu, B. B. Goldberg: In vivo pressure estimation using subharmonic contrast microbubble signals: Proof of concept. IEEE Trans. Ultrason. Ferroelectr. Freq. Control **52** (2005) 581–583.

[8] W. T. Shi, F. Forsberg, J. S. Raichlen, L. Needleman, B. B. Goldberg: Impact of acoustic pressure on ambient pressure estimation using ultrasound contrast agent. Ultrasound Med. Biol. **25** (1999) 275–283.

[9] L. M. Leodore, F. Forsberg, W. T. Shi: In vitro pressure estimation obtained from subharmonic contrast microbubble signals. IEEE International Ultrasonics Symposium Proceedings, 2007, P5B–6.

[10] P. J. A. Frinking, E. Gaud, J. Brochot, M. Arditi: Subharmonic scattering of phospholipid-shell microbubbles at low acoustic pressure amplitudes. IEEE Trans. Ultrason. Ferroelectr. Freq. Contrl **57** (2010) 1762–1771.

[11] K. S. Andersen, J. A. Jensen: Impact of acoustic pressure on ambient pressure estimation using ultrasound contrast agent. J. Acoust. Soc. Am. **126** (2009) 3350–3358.

[12] A. Katiyar, K. Sarkar, F. Forsberg: Modeling subharmonic response from contrast microbubbles as a function of ambient static pressure. J. Acoust. Soc. Am. **129** (2011) 2325–2335.

[13] P. Marmottant, S. van der Meer, M. Emmer, M. Versluis: A model for large amplitude oscillations of coated bubbles accounting for buckling and rupture. J. Acoust. Soc. Am. **118** (2005) 3499.

[14] H. R. Zheng, A. Barker, R. Shandas: Predicting backscatter characteristics from micron- and submicron-scale ultrasound contrast agents using a size-integration technique. IEEE Trans. Ultrason. Ferroelectr. Freq. Contrl. **53** (2006) 639–644.

[15] M. X. Tang, J. Loughran, E. Stride, D. Zhang, R. J. Eckersley: Effect of bubble shell nonlinearity on ultrasound nonlinear propagation through microbubble populations. J. Acoust. Soc. Am. **129** (2011) EL76–82.

[16] L. Hoff, P. C. Sontum, J. Hovem: Oscillations of polymeric microbubbles: Effect of the encapsulating shell. J. Acoust. Soc. Am. **107** (2000) 2272–2280.

[17] N. de Jong, L. Hoff: Ultrasound scattering properties of Albunex microspheres. Ultrasonics **31** (1993) 175–181.

[18] J. F. Yu, D. Zhang, X. F. Gong: Frequency dependences of sound attenuation and phase velocity in suspensions containing encapsulated microbubbles. Chin. Phys. Lett. **22** (2005) 892–895.

[19] Y. J. Gong, D. Zhang, X. F. Gong: Subharmonic and ultraharmonic emissions based on the nonlinear oscillation of encapsulated microbubbles in ultrasound contrast agents. Chinese Science Bulletin **50** (2005) 1975–1978.